International Journal of Fluid Power 8 (2007) No. 1 pp. 17-28

A FREE PISTON COMPRESSOR AS A PNEUMATIC MOBILE ROBOT POWER SUPPLY: DESIGN, CHARACTERIZATION AND EXPERIMENTAL OPERATION

José A. Riofrio and Eric J. Barth

Department of Mechanical Engineering – Vanderbilt University, Nashville, Tennessee, USA
eric.j.barth@vanderbilt.edu

Abstract

The design and dynamic characterization of a free piston compressor (FPC) is presented in this paper. The FPC is a proposed device that utilizes combustion of a hydrocarbon fuel to compress air into a high-pressure supply tank, thus serving as a portable pneumatic power supply for mobile untethered robotic systems. The device is configured such that the transduction from thermal energy to stored energy, in the form of compressed gas, is efficient relative to other small-scale portable power supply systems. This efficiency is achieved by matching the dynamic load of the compressor to the ideal adiabatic expansion of the hot gas combustion products. It is shown that a load that is dominantly inertial provides a nearly ideally matched load for achieving high thermodynamic efficiency in a heat engine. The device proposed exploits this fact by converting thermal energy first into kinetic energy of the free piston, and then compressing air during a separate compressor phase. The proposed technology is intended to provide a compact pneumatic power supply source appropriate for human-scale robots. An analytical model of the proposed device is developed, and an FPC prototype is designed and built and its yielded experimental results are compared with theoretical.

Keywords: free-piston engine, over expansion engine, pneumatic compressor, portable power supply, untethered robots

1 Introduction

The need for an effective portable power supply for human-scale robots has increasingly become a matter of interest in robotics research. Current prototypes of humanoid robots, such as the Honda P3, Honda ASIMO and the Sony QRIO, show significant limitations in the capacity of their power sources in between charges (the operation time of the humanoid-size Honda P3, for instance, is only 20 to 25 minutes). This limitation becomes a strong motivation for the development and implementation of a more adequate source of power. Moreover, the power density of the actuators coupled to the power source needs to be maximized such that, on a systems level evaluation, the combined power supply and actuation system is both energy and power dense. Put simply, state-of-the-art batteries are too heavy for the amount of energy they store, and electric motors are too heavy for the mechanical power they can deliver, in order to present a viable combined power supply and actuation system that is capable of delivering human-scale mechanical work in a human-scale self contained robot package, for a useful duration of time (Goldfarb, et al., 2003).

This manuscript was received on 9 January 2006 and was accepted after revision for publication on 20 February 2007

The total energetic merit of an untethered power supply and actuation system is a combined measure of 1) the source energy density of the energetic substance being carried, 2) the efficiency of conversion to controlled mechanical work, 3) the energy converter mass, and 4) the power density of the actuators. With regard to a battery powered electric motor actuated system, the efficiency of conversion from stored electrochemical energy to shaft work after a gear head can be high (~50%) with very little converter mass (e.g. PWM amplifiers); however, the energy density of batteries is relatively low (about 180 kJ/kg for NiMH batteries), and the power density of electrical motors is not very high (on the order of 50 W/kg), rendering the overall system heavy in relation to the mechanical work that it can output. With regard to the hydrocarbon-pneumatic power supply and actuation approach presented here relative to the battery/motor system, the converter mass is high and the total conversion efficiency is shown to be low. However, the energy density of hydrocarbon fuels, where the oxidizer is obtained from the environment and is therefore free of its associated mass penalty, is in the neighborhood of 45 MJ/kg, which is more

than 200 times greater than the energy density of state of the art electrical batteries. This implies that even with poor conversion efficiency (poor but within the same order of magnitude), the available energy to the actuator per unit mass of the energy source is still at least one order of magnitude greater than the battery/motor system. Additionally, linear pneumatic actuators have approximately an order of magnitude better volumetric power density and a five times better mass specific power density (Kuribayashi, 1993) than state of the art electrical motors. Therefore, the combined factors of a high-energy density fuel, the efficiency of the device, the compactness and low weight of the device, and the use of the device to drive lightweight linear pneumatic actuators (lightweight as compared with power comparable electric motors) is projected to provide at least an order of magnitude greater total system energy density (power supply and actuation) than state of the art power supply (batteries) and actuators (electric motors) appropriate for human-scale power output.

The FPC presented in this paper serves the function of converting chemically stored energy of a hydrocarbon into pneumatic potential energy of compressed air. More specifically, it extracts the energy via combustion of a stoichiometric mixture of propane and air, and the combustion-driven free piston acts as an air pump to produce the compressed air.

The idea of using a free piston combustion-based device as a pump has been around since the original free-piston patent by Pescara (1928). Junkers developed a free piston compressor that became widely used by German submarines through World War II (Nakahara, 2001). The automotive industry conducted a large amount of research in the 1950's. Ford Motor Company considered the use of a free piston device as a gasifier in 1954 (Klotsch, 1959). General Motors presented the "Hyprex" engine in 1957 (Underwood, 1957). Such endeavors were aimed at an automotive scale engine and were largely unsuccessful. In more recent times, the free piston engine concept has been considered for small-scale power generation. Aichlmayr, et al. (2002a, 2002b) have considered the use of a free piston device as an electrical power source on the 10 W scale meant to compete with batteries. Beachley and Fronczak (1992), among others, have considered the design of a free-piston hydraulic pump. McGee, et al. (2004) have considered the use of a monopropellant-based catalytic reaction as an alternative to combustion, as applied to a free piston hydraulic pump.

Despite free piston devices having been studied in the past, none of these previous designs explicitly featured what is perhaps the main advantage of a free piston, which is its capability to offer a purely inertial load. The main focus of this work is to exploit the fact that a free piston can present a purely inertial load to the combustion, and as a result, desirable operational characteristics can be obtained, such as high efficiency, low noise, and low temperature operation. Additionally, this work aims to demonstrate that a free piston compressor stands as a strong candidate for a portable power supply system for untethered human-scale pneumatic robots.

An outline of this paper is as follows. Section 2 describes the proposed device and its operation, and outlines its main features. Sections 3 and 4 present a thermodynamic and dynamic model respectively, a simulation of the system, and its yielded theoretical predictions. Section 5 presents the design and implementation of a bench-top laboratory prototype FPC, and its main design features. Section 5 also shows all relevant experimental data along with their respective analysis and evaluation, and compares experimentally obtained data with theoretical predictions. Finally, section 6 presents the main conclusions and a discussion of the FPC's capability to compete with state-of-the-art power supply technology.

2 The Free Piston Compressor

A generalized schematic of the free piston compressor system is shown in Fig. 1. The device is completely symmetrical, so its starting position can be on either side. The operation of the device is as follows: The piston is held in place by two magnets while injecting a mixture of pressurized air and fuel (propane, in this case) into the combustion chamber. Once the proper amount of mixture has entered the chamber, the air and propane valves close and a sparkplug initiates combustion. The piston will then travel to the other side while serving four functions: (1) pump fresh air into the air reservoir; (2) exhaust the combustion products from the previous combustion out of the opposing cylinder's combustion chamber; (3) breathe in fresh air into the opposing cylinder's pumping chamber; and (4) breathe in fresh air into the combustion chamber after the pressure has dropped below atmospheric, thus cooling down the combustion products. At the end of the stroke the piston will be held in place by the opposing magnets, and the cycle can occur on the opposite side in the same fashion. The work required to break away the magnetic holding force after combustion is retrieved at the end of pumping. The force-distance profile of the magnets also allows dominantly inertial loading presented to the combustion pressure a very short distance after break-away has occurred.

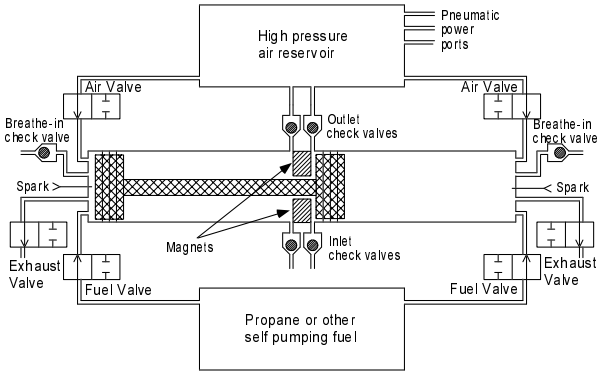

Fig. 1: *Schematic of the free piston compressor system*

As a result of its novel configuration, the FPC offers on-demand start and stop (since there is no compres-

sion stroke in the engine side), cool operation (given that the combustion products are mixed with fresh air after expanding down below atmospheric pressure), quiet operation (given that there is no exhaust of high-pressure gasses), and simplicity (in terms of the number of moving parts relative to modern IC engines). These characteristics are achieved due to the following main features of the FPC (Riofrio and Barth 2005):

Inertial Loading – The free piston is not rigidly attached to a crankshaft or any timing linkage alike, so it offers a purely inertial loading to the expanding combustion gasses. This allows the free piston to store as kinetic energy the work done by the ideal adiabatic expansion of the combustion gasses, and allows full expansion (i.e., over expansion) down to atmospheric pressure. This over expansion contributes to a higher efficiency than if it were not allowed, as is the case with most small-scale IC engines (Fig. 2). Typical IC engines are required to provide a high *immediate* output power profile in their design specifications, so they are concerned only with extracting the higher-power portion of the combustion P-V curve, and wastefully exhaust the rest. The FPC, on the other hand, is decoupled from the main device's (e.g. robot) transient output power demands, since its function is only to store potential energy at an average power rate, and therefore it can extract the lower-power portion of the P-V curve as well. As an additional consequence, the FPC has a quiet exhaust, since no high-pressure gasses are exhausted into the atmosphere.

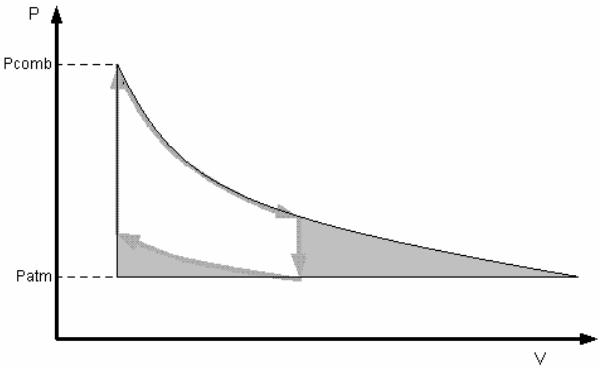

Fig. 2: *P-V diagram of FPC cycle superimposed on a P-V diagram of the Otto cycle. The shaded region to the right represents the additional work extracted in the FPC cycle that is not extracted in the Otto cycle.*

Breathe-in Mechanism – When the combustion gasses reach atmospheric pressure, the free piston will still be traveling (with maximum kinetic energy), and thus will induce a drop of pressure in the combustion chamber as the motion continues. This pressure drop will cause an intake check valve to open and allow fresh atmospheric air to enter the chamber. This fresh air will cool down the combustion products, ensuring a low temperature operation of the device.

Start on Demand – Since the intake valves and spark plugs are electrically actuated, and since high-pressure fuel and air (from the reservoir) injection eliminate the need for conventional intake and compression strokes, the FPC does not require the implementation of a starter. This allows the engine to start on demand, without the need for a separate starting cycle. With regard to typical IC engine metrics, the magnets that hold the piston in place during the injection phase allow a high "compression ratio", and allow for a much greater than 100% "volumetric efficiency" due to the lack of a compression stroke that would otherwise increase the temperature of the pre-combustion gases.

3 Thermodynamic Analysis

Both the thermodynamic and dynamic characteristics of the system were modelled prior to hardware design. From a thermodynamic analysis, the energetic characteristics of the FPC are modelled separately by the engine side (combustion) and the pump side (compression and pumping).

3.1 Engine Side

The engine side converts the energy of combustion into kinetic energy of the free piston, while the compressor side then converts this kinetic energy into stored compressed gas in the high-pressure reservoir. Presenting a purely inertial load during the expansion of the combustion products allows the right loading characteristics such that the high-pressure combustion products are allowed to fully expand down to atmospheric pressure. Assuming an adiabatic process in the combustion chamber immediately following combustion, the work done on the inertial load will be equal to the following:

$$W_{\mathrm{e}} = \frac{P_{\mathrm{e}0}V_{\mathrm{e}0}^{\gamma_{\mathrm{e}}}}{1-\gamma_{\mathrm{e}}}\left(V_{\mathrm{ef}}^{1-\gamma_{\mathrm{e}}} - V_{\mathrm{e}0}^{1-\gamma_{\mathrm{e}}}\right) - P_{\mathrm{atm}}\left(V_{\mathrm{ef}} - V_{\mathrm{e}0}\right) \tag{1}$$

Assuming that losses associated with friction are negligible, the kinetic energy of the piston will be equal to the work done W_{e}, when reaching the position associated with the final volume V_{ef}. It is shown by Barth and Riofrio (2004) that the efficiency of conversion from stored chemical energy of the fuel to kinetic energy of the free piston is given by,

$$\eta_{\mathrm{KE}} = \frac{W_{\mathrm{e}}}{m_{\mathrm{e}0}\mathrm{e}} = \left(\frac{R_{\mathrm{e}}T_{\mathrm{AFT}}}{\mathrm{e}}\right)\left(\frac{\gamma_{\mathrm{e}}P_{\mathrm{e}0}^{1/\gamma_{\mathrm{e}}}P_{\mathrm{atm}}^{(\gamma_{\mathrm{e}}-1)/\gamma_{\mathrm{e}}} - P_{\mathrm{e}0} + (1-\gamma_{\mathrm{e}})P_{\mathrm{atm}}}{(1-\gamma_{\mathrm{e}})P_{\mathrm{e}0}}\right) \tag{2}$$

where e is computed as the following for the air supported combustion of propane:

$$\begin{aligned}\mathrm{e} &= \frac{46350\ \mathrm{kJ}}{\mathrm{kg\ fuel}} \times \frac{1\ \mathrm{kg\ fuel}}{16.63\ \mathrm{kg\ fuel/air\ mixture}} \\ &= 2,787\ \frac{\mathrm{kJ}}{\mathrm{kg\ fuel/air\ mixture}}\end{aligned} \tag{3}$$

3.2 Compressor Side and Reservoir

The compressor side of the FPC holds two separate processes: firstly, the adiabatic (or polytropic) compression of air, and secondly, the constant pressure process of pumping the air into the high-pressure reservoir. As shown by Barth and Riofrio (2004), the work associated with the adiabatic compression process and the constant pressure pumping process are given by the

following,

$$W_{c1} = \frac{P_{atm} V_{c0}^{\gamma}}{1-\gamma}\left(V_{ci}^{1-\gamma} - V_{c0}^{1-\gamma}\right) - P_{atm}\left(V_{ci} - V_{c0}\right) \quad (4a)$$

$$W_{c2} = \left(P_s - P_{atm}\right)\left(V_{cf} - V_{ci}\right) \quad (4b)$$

where V_{cf} is approximated as zero. At the intermediary volume V_{ci}, the air is at a temperature T_{ci} and is being pumped at the constant pressure P_s, which is the pressure in the air reservoir. Once the air is in the reservoir, and assuming that the reservoir is large, at constant pressure, and that the residence time of the air is large, this air will cool to T_{amb}, and undertake its final partial volume, V_f. At this point, the compressed air will take its final form as stored pneumatic potential energy, which, if considered to be its capacity to perform adiabatic work (i.e. in a pneumatic actuator), is given by,

$$E_{stored} = \frac{P_s V_f}{1-\gamma}\left[\left(\frac{P_s}{P_{atm}}\right)^{\frac{1-\gamma}{\gamma}} - 1\right] \quad (5)$$

Since the mass of air is the same at V_{c0}, V_{ci} and V_f, and noting that the pressure and temperature at V_{c0} are P_{atm} and T_{amb}, respectively, we can use ideal gas law expressions to derive the following relationship:

$$V_f = \left(\frac{P_{atm}}{P_s}\right) V_{co} \quad (6)$$

Finally, the efficiency of converting the kinetic energy of the free piston into stored pneumatic potential energy of compressed air is given by,

$$\eta_{PE} = \frac{E_{stored}}{W_e} \quad (7)$$

3.3 Mass Investment

To complete the cycle, the mass of air utilized from the reservoir to support the combustion process must be taken into account. Since the energy stored is proportional to the mass in the reservoir, the investment of air mass needed for the combustion, as shown by Barth and Riofrio (2004), can be expressed as the following efficiency,

$$\eta_{invest} = \frac{m_c - \frac{15.63}{16.63} m_{e0}}{m_c} = 1 - \frac{15.63}{16.63}\frac{P_{e0} V_{e0} R T_{amb}}{P_{atm} V_{c0} R_e T_{AFT}} \quad (8)$$

where the functionally constrained volume ratio of initial combustion chamber volume to initial compressor chamber volume, V_{e0}/V_{c0}, required to match the peak kinetic energy to the work of compression and pumping, is:

$$\frac{V_{e0}}{V_{c0}} = \frac{\frac{\gamma P_{atm}}{(1-\gamma)}\left[1 - \left(\frac{P_{atm}}{P_s}\right)^{\frac{1-\gamma}{\gamma}}\right]}{\frac{P_{e0}}{(1-\gamma_e)}\left[\gamma_e\left(\frac{P_{atm}}{P_{e0}}\right)^{\frac{\gamma_e - 1}{\gamma_e}} - 1 + (1-\gamma_e)\left(\frac{P_{atm}}{P_{e0}}\right)\right]} \quad (9)$$

3.4 System Efficiency

The overall efficiency of the system can be found by multiplying the individual efficiencies η_{KE}, η_{PE}, and η_{invest}. By multiplying Eq. 2, 7 and 8, and substituting Eq. 5, 6 and 9, the overall system efficiency, assuming full expansion to atmospheric pressure in the combustion chamber, is found in closed-form as follows:

(See Appendix) (10)

Figure 3 shows the overall system efficiency as a function of the initial combustion pressure for various reservoir pressure values.

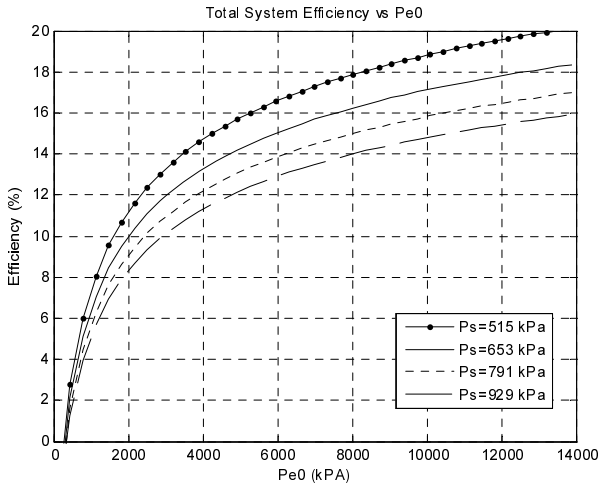

Fig. 3: *The overall system efficiency as a function of the initial combustion pressure (for various values of Ps).*

As pointed out earlier, the overall efficiency of the FPC is small relative to a battery powered electric motor actuated system. However, this efficiency, while smaller than that in the electrical domain, is adequate enough to provide at least an order of magnitude greater total system energy density by exploiting the high energy density of hydrocarbon fuels.

4 Dynamic Model

While a thermodynamic model was developed to predict the total system efficiency, a dynamic model was likewise obtained in order to characterize the time-based behavior of the system. Immediately following combustion, the pressure and temperature dynamics in the combustion side are determined by the following power balance:

$$\dot{U}_e = \dot{H}_e + \dot{Q}_e - \dot{W}_e \quad (11)$$

Assuming an ideal gas, the rate of internal energy storage is given by the following two relationships:

$$\dot{U}_e = \dot{m}_e c_{ve} T_e + m_e c_{ve} \dot{T}_e = \frac{1}{\gamma_e - 1}(\dot{P}_e V_e + P_e \dot{V}_e) \quad (12)$$

The values of c_{ve} and γ_e must in general be found from the appropriately weighted average of the temperature dependent values of c_p of the species contained within the chamber. The enthalpy rate of energy entering or exiting the control volume is given by:

$$\dot{H}_e = \dot{m}_e c_{p,in/out} T_{in/out} \quad (13)$$

If it is assumed that the engine side is adiabatic, then $\dot{Q}_e = 0$. The work rate is given as:

$$\dot{W}_e = P_e \dot{V}_e \quad (14)$$

The operation of the "engine side" of the device can be considered in three phases: the work phase (described below), and the intake and exhaust phases (described in Barth and Riofrio (2004)).

During the work phase, no mass flow occurs and Eq. 11-14 reduces to the following relationships regarding the pressure and temperature dynamics inside the combustion chamber:

$$\dot{P}_e = \frac{-\gamma_e P_e \dot{V}_e}{V_e} \quad (15)$$

$$\dot{T}_e = \frac{-P_e \dot{V}_e}{m_{e0} c_{ve}} \quad (16)$$

The work phase persists while $P_e > P_{atm} - P_{cvd}$.

The dynamics in the engine side and the compressor side are related to each other through the movement of the free piston. Neglecting viscous and Coulomb friction, and neglecting the slight pressure variations in the opposing side needed to push out exhaust product in the opposing combustion chamber and breathe in air into the opposing pumping chamber, the dynamics of motion of the free piston are given by:

$$M\ddot{x} = (P_e - P_{atm})A_e - (P_c - P_{atm})A_c \quad (17)$$

The volumes of the combustion chamber and compressor chamber (and their associated derivatives) are given by the following:

$$V_e = A_e x \quad (18)$$

$$V_c = A_c (l_c - x) \quad (19)$$

A dynamic simulation of the system was performed using Simulink. The following parameters were used for the simulation: M = 250 g, $A_e = 5.07$ cm^2, $A_c = 2.85$ cm^2, $P_{e0} = 3548$ kPa, $P_{cvd} = 2.3$ kPa, and $P_s = 653$ kPa. The portion of the simulation relating the work phase in the combustion chamber with the inertial dynamics of the free piston is sufficient to model the post-combustion pressure profile (Fig. 4). This profile shows that the combustion gasses are allowed to adiabatically expand all the way down to atmospheric pressure, whereupon the intake check valve opens allowing the combustion products to mix with cool air. This over expansion is essential for the inertial loading characteristic of the FPC, and as it can be seen, it occurs within a very short duration of time, indicating a rapid transduction from stored chemical to kinetic energy. This rapid transduction helps mitigate the effect of heat loss through the combustion chamber wall and enhances efficiency.

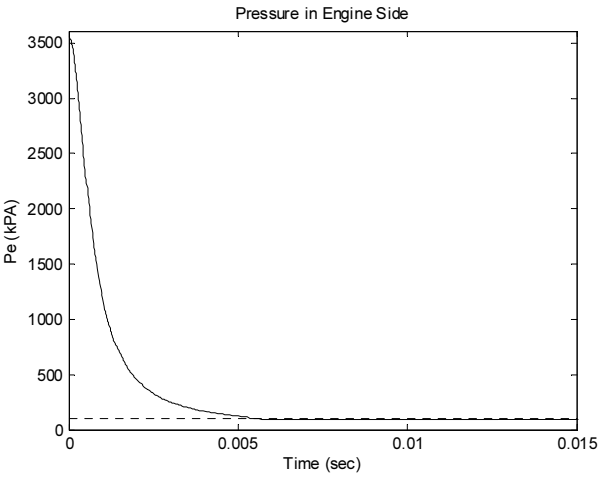

Fig. 4: *Simulated pressure drop in engine side right after combustion.*

5 Design and Implementation

A bench-top prototype of the FPC was built using off-the-shelf pneumatic equipment. The prototype consists of two cylinders in-line and opposing one another. Both cylinders have a combustion side (back of the piston) and a pumping side (rod side of the piston). Figure 5 shows a picture of this prototype, and Fig. 6 shows a close-up of one of the cylinders. The setup of the FPC consists of two 4-inch stroke, ¾-inch bore BIMBA® standard air cylinders, ported appropriately for all necessary flow. The two piston rods are connected to a moving mass with small pieces of plastic tubing in order to avoid a purely rigid connection, which would yield increased friction due to misalignments. For all fluid flow purposes, standard check valves, 2-way on/off valves and 4-way valves were used where needed.

For experimental purposes, the air injected into the combustion chamber is supplied from an external source, and not from the air reservoir that is being pressurized. In an eventual full implementation of a FPC system, the air reservoir would be pre-pressurized at some target high-pressure (i.e., a pressure under which the pneumatic actuators are designed to operate). The FPC would then maintain this pressure by starting on demand, as soon as this pressure begins to drop. Also, in this eventual system, the air used for injection would come directly from the reservoir, which is feasible since the pressure in the reservoir will always be higher than the target injection pressure.

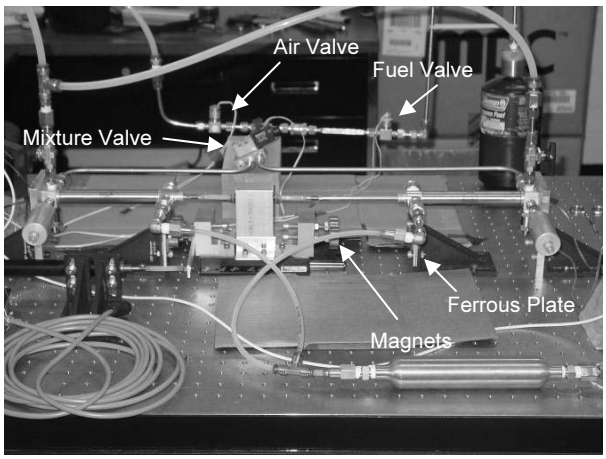

Fig. 5: *Picture of FPC prototype*

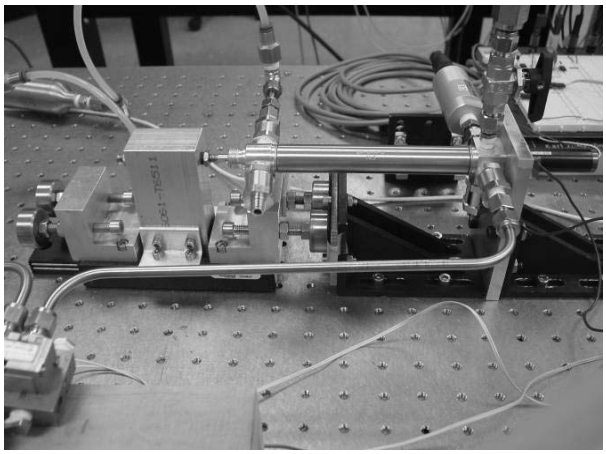

Fig. 6: *Close-up Picture of Cylinder*

5.1 Injection Pressure

In order to obtain desirable combustion characteristics, the injection pressure of the air/fuel mixture needs to be adequate enough to achieve the target initial combustion pressure P_{e0}. This minimum injection pressure requirement is given by,

$$P_{inj} = \left(\frac{R_{mix} T_{inj}}{R_e T_{AFT}} \right) P_{e0} \tag{20}$$

To meet this injection pressure requirement, the four neodymium-iron-boron magnets were mounted onto the moving mass in order to hold the free piston in its starting position before combustion. The magnetic gap is adjustable such that the bonding magnetic force can be set just slightly higher than the force exerted on the free piston by the injection pressure.

5.2 Air/Fuel Mixture

In addition to adequate injection pressure, proper combustion requires a good air/fuel mixture quality. Ideally, this mixture should match the stoichiometric mass ratio for combustion, namely 15.67 for air and propane. In order to ensure such stoichiometry, a separate experiment was performed in which air and propane were separately injected at constant pressure into an inverted graduated cylinder in a beaker initially full of water, for various valve pulse durations. The average water displacement (per pulse and per substance) provided a direct mapping between valve pulse duration and its respective mass flow.

For precise data acquisition purposes, the engine was run only in single fire shots with a constant pressure source of air instead of feeding back the reservoir air (repeated firing and continuous operation was demonstrated in an earlier prototype (Riofrio and Barth 2005)). Before each firing, the exhaust port and mixture valve were opened, and the fuel and air valves opened for specific durations previously determined to yield stoichiometric mixtures. This was done several times such that the entire mixture line (see Fig. 5) would contain a precise air-fuel ratio. The exhaust port was then closed and some of the stoichiometric air/fuel mixture remaining in the mixture line was pushed into the combustion chamber, by pulsing the injection valves, until reaching the desired injection pressure. It was ensured that the mixture line was long enough such that only a portion of the line was required for injection, and thus maintaining a proper mixture. The fuel injection process can be considered an adiabatic compression, as follows:

$$P_{atm} V_{line}^{\gamma_{mix}} = P_{inj} V_{e0}^{\gamma_{mix}} \tag{21}$$

Additionally, by conservation of mass, and assuming an ideal gas, we have:

$$m_{e0} = \frac{P_{atm} V_{line}}{R_{mix} T_{amb}} = \frac{P_{inj} V_{e0}}{R_{mix} T_{inj}} \tag{22}$$

Combining Eq. 21 and 22, the injected mass of fuel can be calculated as:

$$m_{e0} = \frac{P_{atm} V_{e0}}{R_{mix} T_{room}} \left(\frac{P_{inj}}{P_{atm}} \right)^{\frac{1}{\gamma_{mix}}} \tag{23}$$

5.3 Experimental Results and Evaluation

Combustion took place in a 6.4 mL volume, with a moving mass of 1.82 kg. Assuming stoichiometric mixtures, the dimensionless specific heat ratios γ, γ_e and γ_{mix} are calculated to be 1.398, 1.249 and 1.366, respectively. Figures 7, 8, 9 and 10 show combustion pressure, air reservoir pressure, position of the piston and velocity of the piston, respectively. These were taken from a typical firing at a low pumping pressure and exhibit the inadequacy of resolution of the air and fuel valves – note the collision with the opposing side apparent from the sharp decrease in velocity shown in Fig. 10. The spark occurs at 0.4 seconds. Figure 7 also shows the injection pressure in the combustion chamber before ignition.

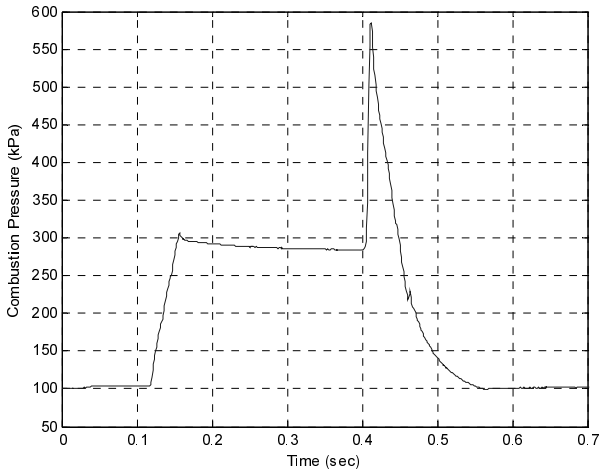

Fig 7: *Experimental pressure in the combustion chamber. fuel injection occurs between 0.1 and 0.2 seconds; spark ignites at 0.4 seconds.*

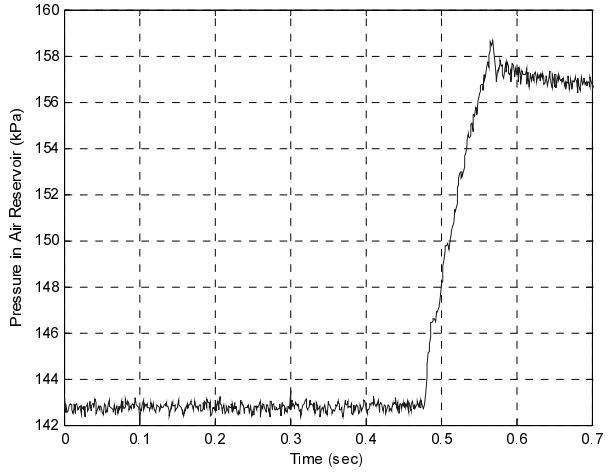

Fig. 8: *Experimental pressure in the air reservoir*

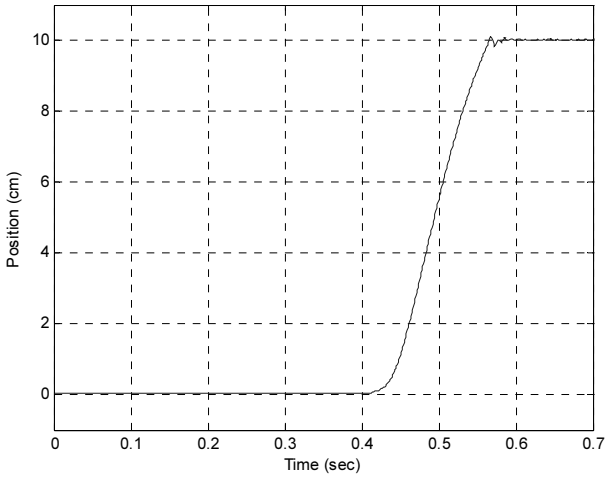

Fig. 9: *Experimental position of the free piston. Sharp corner at the top indicates abrupt collision of piston with magnets (loss of energy).*

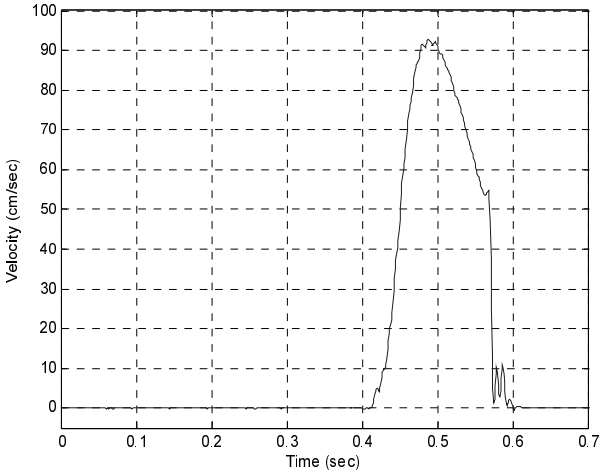

Fig. 10: *Experimental velocity of the free piston. Vertical line at the right indicates wasted kinetic energy.*

Despite the inefficient operation due to overloading the free piston with excessive kinetic energy for the pumping work required (essentially a violation of Eq. 9), it should be noted that these plots still exhibit the main features of the FPC, such as the inertial loading (over expansion of combustion gasses in Fig. 7) and the breathe-in mechanism (combustion pressure decreases to atmospheric pressure before the end of the stroke).

An evaluation of the experimentally obtained P-V curve, shown in Fig. 11, compares the experimental prototype device with the theoretically adiabatic behaviour of $PV^{\gamma_c} = \text{constant}$. It can be seen that the experimentally obtained curve becomes flat at atmospheric pressure and indicates that the device is capable of both fully expanding the combustion products as well as being able to intake cool air from the environment to cool the exhaust products. In light of this comparison, heat loss, leakage and other non-ideal effects appear to be non-negligible but manageable. It should be noted that the curve shown is from the device firing the first time when the device is cold and when heat losses would be at a maximum. Heat losses can be further reduced by choosing a different material for the combustion chamber walls (currently aluminum) and increasing the combustion dead volume (which would increase the ratio of volume to surface area).

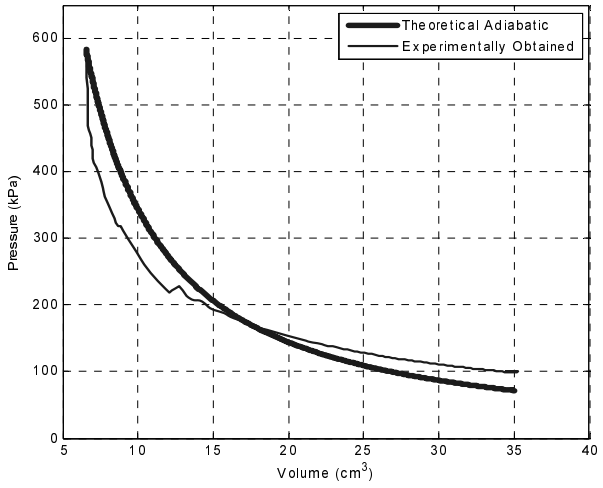

Fig. 11: *P-V curve in the combustion chamber*

Through single fire shots, the 187 mL air reservoir was successfully compressed from atmospheric pressure up to 310 kPa. This compression pressure is limited by the ratio of stroke volume (engine displacement) over dead volume in the rod (compressing) side of the chosen cylinders. This dead volume was quite large (about 4.1 mL), and is a nonideality that should be reduced in future design considerations. This nonideality presents the main drawback in this particular FPC bench-top prototype.

The total energetic merit of this system is represented by the efficiency of conversion from chemically stored energy in propane to pneumatic potential energy of compressed air. Experimentally, this efficiency was calculated for a single fire shot in which the piston just "barely made it" to the other side – the ideal case which could conceivably be achieved for every stroke given adequate valve resolution. Figures 12, 13, 14 and 15 show the respective pressures, displacement and velocity for this particular shot. By looking at the position and velocity, it can be observed that the piston "barely made it" to the other side, with a little help from the magnetic force.

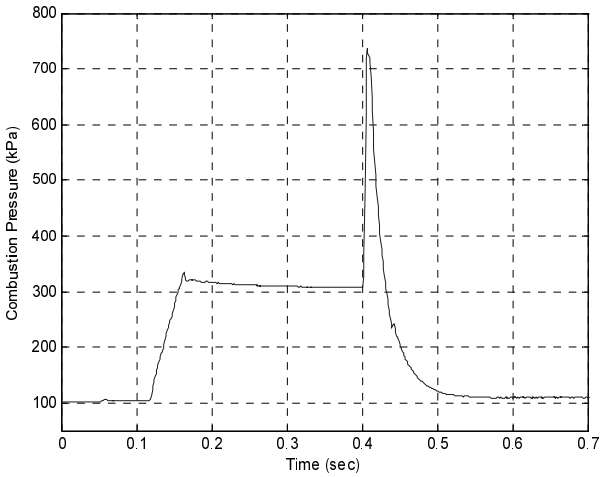

Fig. 12: *Experimental pressure in the combustion chamber for efficient firing*

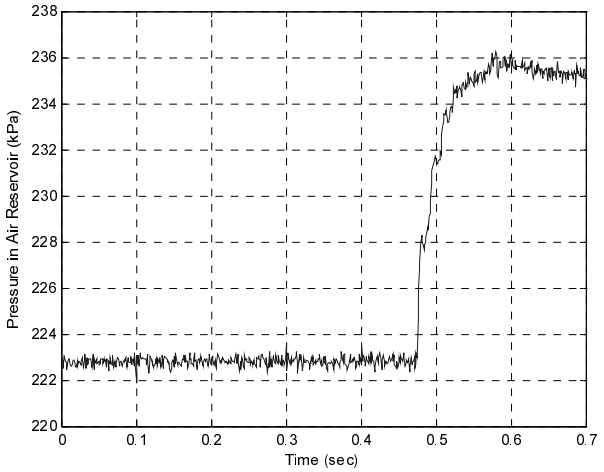

Fig. 13: *Experimental pressure in the air reservoir*

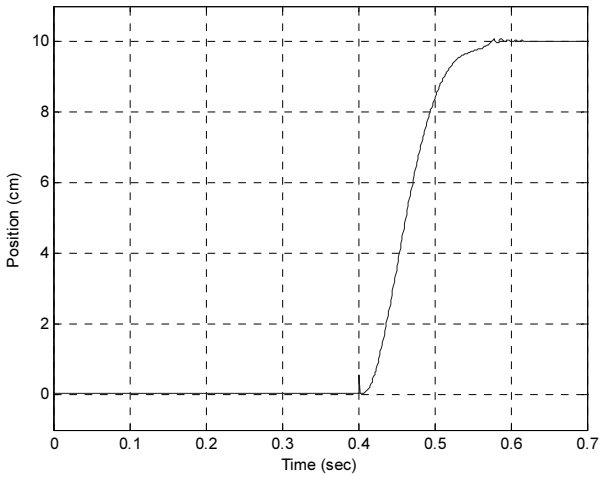

Fig. 14: *Experimental position of the free piston. smooth curve at the top indicates that piston "barely made it" to the other side.*

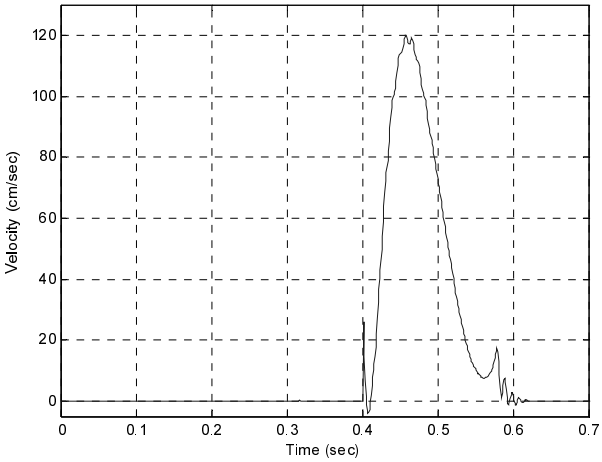

Fig. 15: *Experimental velocity of the free piston. Spike at the bottom-right shows the piston snapping into the magnets, hence an efficient firing.*

The firing displayed in Figs. 12-15 used 1.05×10^{-6} kg of propane and resulted in an increase of the pressure in the air reservoir (a volume of 1.866×10^{-4} m^3) from 222.75 kPa to 235 kPa. Using Eq. 5, the pneumatic potential energy increase is calculated as 2.48 Joules. The total efficiency of conversion from chemically stored energy of the fuel to stored pneumatic energy of the compressed air, is calculated as,

$$\eta_{\text{total}} = \frac{0.00248337\ \text{kJ}}{\frac{46350\ \text{kJ}}{\text{kg fuel}}\times 1.05*10^{-6}\ \text{kg fuel}}\times 100 = 5.10\% \quad (24)$$

Additionally, to calculate the overall system efficiency, we need to take into account the efficiency associated with the air re-investment; that is, the air from the reservoir that is utilized for the subsequent combustion cycle. Using Eq. 8, this efficiency can be calculated as,

$$\eta_{\text{invest}} = \frac{2.69\times10^{-5} - 1.645*10^{-5}}{2.69\times10^{-5}}\times 100 = 39\% \quad (25)$$

Hence, the overall system efficiency of this shot becomes,

$$\eta_{sys} = \eta_{total}\eta_{invest} = 1.99\%$$

A useful way to verify the efficiency obtained in Eq. 24 is by examining the PV diagram of the pumping side, shown in Fig. 16. This diagram had to be partially reconstructed due to the absence of a pressure signal from the chamber. The effective work delivered to the air reservoir is represented by the area under the curve, minus the area below the atmospheric pressure line. It should be noted that the amount of work corresponding to the compression portion of the curve may be wasted by the pneumatic actuator down the line. However, this waste should be accounted for by the low efficiency of pneumatic actuators, assumed to be about 30%. An overall systems-level energetic merit discussion is provided below, which addresses this point in a more practical context.

The area under the curve in Fig. 16 was calculated as 2.173 J. The small discrepancy between this value and the value calculated directly from the air reservoir is mostly due to the lack of an experimental pressure signal during compression (reconstructed as isothermal), and also due to possible inaccuracies in measured quantities, especially of dead volumes. Since such inaccuracies are less consequential in the air reservoir control volume (due to its larger size), and since all the data corresponding to the reservoir was obtained experimentally, we give preference to the more precise efficiency values obtained in Eq. 24 and 25.

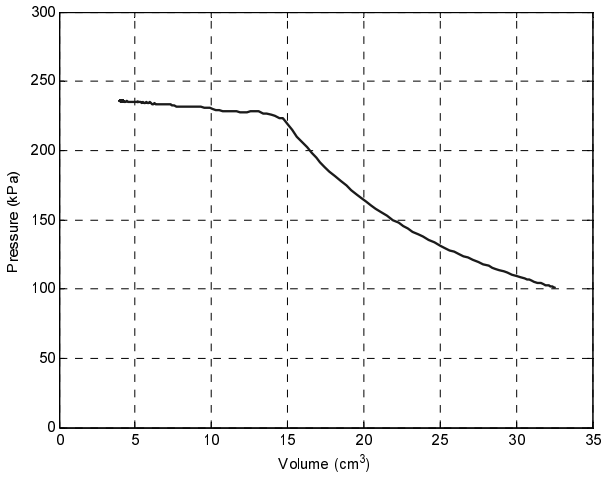

Fig. 16: *Reconstructed PV diagram of the pumping side. The curve on the right side represents an assumed isothermal compression of the air, while the almost-flat section at the top-left (obtained experimentally) shows the pumping process (i.e., compressed air being delivered to the reservoir).*

Based on the thermodynamic analysis presented by Barth and Riofrio (2004), the total theoretical efficiency of the system with these parameters is calculated to be 5.19%. However, this calculation assumes zero dead volume in the pumping side of the cylinder, no heat losses in the combustor side and high heat losses in the compressor side (advantageous to efficiency if the reservoir is assumed to lose heat). The issues of excess dead volume in the compressor side and combustor heat losses present in this experimental prototype would be difficult to fully address with standard pneumatic equipment (such as those used here), and would require custom made parts in order to reduce the minimum rod-side volume, increase the combustor volume (without sacrificing stroke length), and use a better insulating material for the combustor walls. As also shown in Fig. 3, the efficiency of the device increases with increased combustion pressure (up to 20% efficiency). With these points in mind, the obtained experimental efficiency met reasonable expectations, while leaving room for improvement in future designs.

Aside from a proper energetic merit, a power supply of this nature needs to have high enough power density to keep up with the actuator demands. The power density is calculated as the product of the net energy delivered to the reservoir (per cycle) by the frequency of operation of the device. With the specific hardware and experimental operational parameters used in this work, the achievability of a high power density cannot be experimentally demonstrated (since the net energy delivered to the reservoir was approximately 2.5 Joules). The work presented in this paper aimed to focus exclusively on addressing the efficiency of the device, and hence its overall energetic merit. To thoroughly address power density, many design issues will need to be considered. These include: reducing the dead volume in the pump side of the cylinder, slightly increasing the volume in the combustion chamber and properly insulating its walls, increasing the combustion pressure to about 2500 kPa, increasing the frequency of operation by shortening the durations between signals, and adding one or more cylinders (which consequentially would reduce vibration). These design changes will not adversely affect the efficiency of the device or the energetic merits discussed in the paper. It should be pointed out that utilizing an over expanded cycle does have the effect of lowering the power density of the device for the sake of increasing efficiency, essentially because it takes longer to capture the tail end of the P-V work transduction, but since achieving an adequate power density is the aim, as opposed to optimizing the power density, this should not cause difficulty. The issue of designing for adequate power density while maintaining the other energetic merits mentioned is intended to be fully addressed in future work.

6 Conclusions

The design, characterization and experimental operation a Free Piston Compressor (FPC) was presented. The FPC is a small-scale internal combustion engine capable of pumping air into a high-pressure air reservoir, and is intended to serve as a portable pneumatic power supply for untethered pneumatic robots. The proposed technology aims to provide an order of magnitude greater energetic merit than state of the art power supply and actuation systems (electrical batteries coupled with DC motors).

Experimental results demonstrate that the device is capable of fully expanding the combustion products down to atmospheric pressure as designed and demonstrate the merits of presenting a purely inertial load in a

combustion process. Such dynamic loading serves to increase efficiency, allows the device to operate with low noise due to not having a high pressure exhaust "pop", and allows the combustion products to be mixed with cool external air to contribute toward a low operating temperature compared to more conventional internal combustion engines. Experimental results also demonstrate that the device is capable of start-on-demand, making it well suited to a pressure regulation control loop in a portable pneumatic power supply system. An overall measured efficiency of 1.99% was achieved in converting stored chemical energy of propane into stored pneumatic potential energy. In comparing this power supply system with state of the art rechargeable batteries, an energy density of 180 kJ/kg for NiMH batteries and a conversion efficiency of 50% for an electromagnetic motor and mated gearhead would yield 90 kJ of delivered controlled mechanical work per kilogram of source energetic material. For the FPC under consideration, an energy density of 46350 kJ/kg for propane, a measured conversion efficiency of 5.10% from stored chemical to pneumatic energy, a 39% efficiency associated with the computed mass reinvestment from the air reservoir for the next combustion event, and an assumed conversion efficiency of 30% from stored pneumatic energy to delivered controlled mechanical work of an associated pneumatic actuator (Blackburn, Reethof and Shearer, 1960), would yield a projected 277 kJ of controlled work per kilogram of source energetic material. This increase, coupled with the equally important high power density of pneumatic actuators over electromagnetic motors, should contribute to a power supply and actuation system more appropriate for untethered human scale and power comparable robots and actuated devices. Table 1 (appendix) shows an energetic comparison between conventional rechargeable batteries and the FPC system. It should be noted that the theoretical conversion efficiency (5.2%) corresponds only to the specific parameters from the experimental data (combustion pressure and pressure in the air reservoir, namely), and can significantly increase as shown in Fig. 3. It is also expected that design changes to the next generation of this device will result in further improvements.

Nomenclature

A_c	area of piston (pumping side)	[m^2]
A_e	area of piston (engine side)	[m^2]
$c_{p,in/out}$	constant-pressure heat capacity of the gas entering or exiting combustion chamber	[kJ/kg/K]
c_{ve}	constant-volume heat capacity of combustion products	[kJ/kg/K]
e	mass specific energy of fuel/air mixture	[kJ/kg]
γ	ratio of specific heats of air	
γ_e	ratio of specific heats of combustion products	
γ_{mix}	ratio of specific heats of air/fuel mixture	
$\dot{H}_e$	rate of enthalpy crossing CV	[kJ/s]
l_c	initial length of compressor chamber	[m]
m_{e0}	mass of fuel/air mixture	[kg]
$\dot{m}_e$	mass flow rate into combustion chamber	[kg/s]
M	mass of free piston	[kg]
P_{atm}	atmospheric pressure	[kPa]
P_{cvd}	intake check valve cracking pressure	[kPa]
P_e	pressure in combustion chamber	[kPa]
P_{e0}	initial combustion pressure	[kPa]
P_s	pressure in the air reservoir	[kPa]
$\dot{Q}_e$	heat flux rate into or out from the CV	[kJ/s]
R_e	average gas constant of combustion products	[kJ/kg/K]
R_{mix}	average gas constant of air/fuel mixture	[kJ/kg/K]
T_{AFT}	adiabatic flame temperature	[K]
T_{amb}	ambient temperature	[K]
T_{ci}	temperature of air at intermediate volume V_{ci}	[K]
T_e	temperature of combustion products	[K]
$T_{in/out}$	temperature of gas entering or exiting combustion chamber	[K]
T_{inj}	temperature of air/fuel mixture immediately before combustion	[K]
$\dot{U}_e$	rate of internal energy stored in the combustion control volume	[kJ/s]
V_{c0}	initial volume of compression chamber (where compression begins)	[m^3]
V_{cf}	final (dead) volume of compression chamber	[m^3]
V_{ci}	intermediate volume of compression chamber (where pumping begins)	[m^3]
V_e	volume in combustion chamber	[m^3]
V_{e0}	initial volume in combustion chamber	[m^3]
V_{ef}	final volume in combustion chamber	[m^3]
V_f	final partial volume of pumped air	[m^3]
V_{line}	partial volume of air/fuel mixture before entering combustion chamber	[m^3]
$\dot{W}_e$	work rate in combustion chamber	[kJ/s]
x	position of free piston	[m]

References

Aichlmayr, H. T., **Kittelson, D. B.** and **Zachariah, M. R.** 2002a. Miniature free-piston homogenous charge compression ignition engine-compressor concept – Part I: performance estimation and design considerations unique to small dimensions, *Chemical Engineering Science*, 57, pp. 4161-4171.

Aichlmayr, H. T., **Kittelson, D. B.** and **Zachariah, M. R.** 2002b. Miniature free-piston homogenous charge compression ignition engine-compressor concept – Part II: modeling HCCI combustion in small scales with detailed homogeneous gas phase chemical kinetics, *Chemical Engineering Science*, 57, pp. 4173-4186.

Barth, E. J. and **Riofrio, J.** 2004. Dynamic Characteristics of a Free Piston Compressor, *2004 ASME International Mechanical Engineering Congress and Exposition (IMECE).* Anaheim, CA.

Beachley, N. H. and **Fronczak, F. J.** 1992**.** Design of a Free-Piston Engine-Pump, *SAE Technical Paper Series*, 921740, pp. 1-8.

Blackburn, J. v F., **Reethof, G.** and **Shearer, J. L.** *Fluid Power Control*, Massachusetts: The Massachusetts Institute of Technology, 1960.

Goldfarb, M., **Barth, E. J.**, **Gogola, M. A.** and **Wehrmeyer, J. A.** 2003. Design and Energetic Characterization of a Liquid-Propellant-Powered Actuator for Self-Powered Robots, *IEEE/ASME Transactions on Mechatronics*, Vol. 8, no. 2, pp. 254-262.

Klotsch, P. 1959. Ford Free-Piston Engine Development, *SAE Technical Paper Series*, 590045, Vol. 67, pp. 373-378.

Kuribayashi, K. 1993. Criteria for the evaluation of new actuators as energy converters, *Advanced Robotics*, Vol. 7, no. 4, pp. 289-37.

McGee, T. G., **Raade, J. W.** and **Kazerooni, H.** 2004. Monopropellant-Driven Free Piston Hydraulic Pump for Mobile Robotic Systems, *ASME Journal of Dynamic Systems, Measurement, and Control*, Vol. 126, pp. 75-81.

Nakahara M. 2001. Free Piston Kikai-Kouzou to Rekisi, *Shinko-Techno Gihou*, Vol.13, No.25 & 26.

Pescara, R. P. 1928. Motor Compressor Apparatus, *U.S. Patent* No. 1,657,641.

Riofrio, J. A. and **Barth, E. J.** 2005a. Design of a Free Piston Pneumatic Compressor as a Mobile robot Power Supply, *Proceedings of the 2005 IEEE International Conference on Robotics and Automation (ICRA),* pp. 236-241, Barcelona, Spain.

Underwood, A. F. 1957. The GMR 4-4 'Hyprex' Engine: A Concept of the Free-Piston Engine for Automotive Use, *SAE Technical Paper Series*, 570032, Vol. 65, pp. 377-391.

Appendix

Overall system efficiency:

$$\eta_{sys} = \left(\frac{1}{e}\right)\left(\frac{1}{1-\gamma}\right)\left[\left(\frac{P_s}{P_{atm}}\right)^{\frac{1-\gamma}{\gamma}} - 1\right]\left[\frac{\left(\frac{1}{1-\gamma_e}\right)\left[\gamma_e\left(\frac{P_{atm}}{P_{e0}}\right)^{\frac{\gamma_e-1}{\gamma_e}} - 1 + (1-\gamma_e)\left(\frac{P_{atm}}{P_{e0}}\right)\right]}{\left(\frac{\gamma}{1-\gamma}\right)\left[1-\left(\frac{P_{atm}}{P_s}\right)^{\frac{1-\gamma}{\gamma}}\right]} R_e T_{AFT} - \frac{15.63}{16.63} R_{air} T_{amb}\right] \tag{10}$$

Table 1: Energetic comparison between FPC system, at the particular experimental values of combustion and air reservoir pressures used, and state of the art rechargeable batteries.

System	Source Energy Density (kJ/kg)	Conversion Efficiency	Actuation Efficiency (stored to delivered mechanical work)	Controlled Delivered Mechanical Work (kJ/kg)
Batteries	180	100% (PWM)	50% (Gearhead & Friction)	90
FPC (Theory)	46350	5.20%	30% (Pneumatic Actuator)	725 (8 times batteries)
FPC (Experimental)	46350	2.0%	30% (Pneumatic Actuator)	277 (3 times batteries)

Eric J. Barth
received the B. S. degree in engineering physics from the University of California at Berkeley, and the M. S. and Ph. D. degrees from the Georgia Institute of Technology in mechanical engineering in 1994, 1996, and 2000 respectively. He is currently an assistant professor of mechanical engineering at Vanderbilt University. His research interests include design, modelling and control of fluid power systems, and actuator development for autonomous robots.

José A. Riofrio
received the B. S. degree in engineering physics from Elizabethtown College, PA, and the M. S. in mechanical engineering from Vanderbilt University in 2003 and 2005 respectively. He is currently a Ph.D. candidate at Vanderbilt.